EEEE3083

Power Electronic Applications and Control

Coursework 1: Average Design and Modelling

STUDENT NAME: **Kexin Yu**

ID NUMBER: **20320941**

DATE: **30/11/2023**

This report focuses on the design of the inverter and is divided into 7 sections to present the design methodology, validation results, conclusion and references used in the different parts.

1. Filter Design and Inverter voltage Evaluation

The main objective of this section is to design, evaluate and validate LR filter suitable for inverter. There are three subsections, and the first part is to design an LR filter that can effectively reduce the inverter output current ripple. The second part is a quantitative analysis to evaluate the performance of the filter in the overall system. This involves accurate calculations of the inverter voltage versus current to ensure that the voltage output meets established performance criteria. Finally, the results of the design are verified by simulation in PLECs.

1.1 Design LR filter (Choose appropriate L and R)

The output of an inverter usually contains ripple components of the AC current. To reduce these ripples and thus smooth the output current, an LR filter is used here.

The value of L for this filter should be chosen to be as small as possible to meet the filtering requirements while being able to transmit the required active and reactive power. This means that the selected L can generate sufficient voltages at the switching frequency of the inverter and keep the current ripple within the permissible range. Here the peak-to-peak ripple is related to L using a worst-case design approach based on the required harmonic attenuation of the AC grid current. [1] Eqn 1.1 describes the relationship between the voltage across the inductor (V) and the rate of change of the current (I) in the inductor.

$$V = L\frac{dI}{dt} \qquad \textbf{Eqn 1.1}$$

During one half cycle of the inverter, the current undergoes a complete peak-to-peak variation, so that the current changes from its minimum to its maximum value in one quarter of a switching cycle. The amount of current variation during this quarter cycle can be approximated as the peak-to-peak value of the AC current ripple (ΔI). According to Eqn 1.1, ΔI can be related to the peak voltage across the inductor, thus Eqn 1.2 is written out. Eqn 1.2 shows that ΔI is maximum when the average inverter voltage crosses ($V_{DC}/2$) in a quarter of the period ($T_s/4$). This equation can be further changed to be based on the inverter switching frequency ($f_{sw} = 1/T_s$).

Based on the design specification, AC current ripple (peak-peak) (ΔI) is 0.2 A, DC voltage (V_{DC}) is 600 V, inverter switching frequency (f_{sw}) is 20 kHz, the value of L can be calculated as:

$$\Delta I = \frac{V_{DC}}{2}\frac{1}{L}\frac{(\frac{T_S}{2})}{2} \rightarrow L = \frac{T_S V_{DC}}{8\Delta I} \rightarrow L = \frac{V_{DC}}{8 f_{sw}\Delta I} \qquad \textbf{Eqn 1.2}$$

$$L = \frac{600\ \text{V}}{8\times 20\ \text{kHz}\times 0.2\ \text{A}} = 18.75\ \text{mH}$$

The loss of an inductor at rated power is the power dissipation of its equivalent series resistance, which is 0.25% of rated power. Thus, the value of the series resistance (R) can be calculated using Eqn 1.3. Rated power (P) is 3kW. I_{AC} is the AC RMS current, it can be calculated by Eqn 1.4, where AC RMS voltage (V_{AC}) is 240 V.

$${I_{AC}}^2 R = 0.25\%\ P \rightarrow\ R = \frac{0.25\%\ P}{{I_{AC}}^2} \qquad \textbf{Eqn 1.3}$$

$$I_{AC} = \frac{P}{V_{AC}} = \frac{3\ \text{kW}}{240\ \text{V}} = 12.5\ \text{A} \qquad \textbf{Eqn 1.4}$$

$$R = \frac{0.25\% \times 3\ \text{kW}}{(12.5\ \text{A})^2} = 0.048\ \Omega$$

1.2 Passive effects on the circuit variables

To drive the current in the AC grid and exchange the required active and reactive power, the voltage of the inverter needs to be calculated. To calculate this value immediately, here transfer to the phase domain. Here, reactive power is defined as 0, which means that the AC current is always in phase with the AC voltage. Figure 1.1 shows the simple schematic of the inverter circuit. Figure 1.2 shows the phasor diagram based on this assumption. The relationship between the inverter voltage ($\tilde{V}_{INV}$), AC voltage ($\tilde{V}_{AC}$), and AC current ($\tilde{I}_{AC}$) in the figure can be expressed as Eqn 1.5. Z is the total impedance of the filter, which can be calculated through Eqn 1.6. AC voltage ($\tilde{V}_{AC}$) is defined as a reference, so the phasor of AC voltage ($\tilde{V}_{AC}$) and AC current ($\tilde{I}_{AC}$) can be expressed as $240\angle 0^{\circ}$ and $12.5\angle 0^{\circ}$. With these values, the inverter voltage ($\tilde{V}_{INV}$) can be calculated as follows:

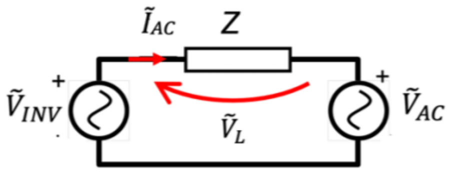

Figure 1.1: The schematic diagram of inverter circuit

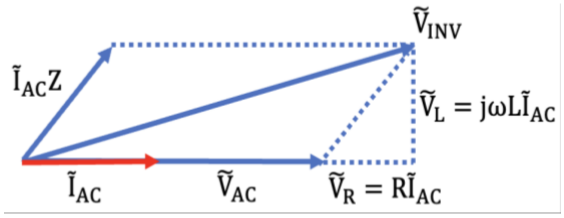

Figure 1.2: The phasor diagram for voltage and current

$$\tilde{V}_{INV} = \tilde{V}_{AC} + \tilde{I}_{AC}Z \qquad \textbf{Eqn 1.5}$$

$$Z = R + j\omega L = R + j2\pi f L \qquad \textbf{Eqn 1.6}$$

$$Z = 0.048\ \Omega + \text{j}2\pi \times 50\ \text{Hz} \times 18.75\ \text{mH} = 0.048 + j5.89 = 5.89\angle 89.53^{\circ}$$

$$\tilde{V}_{INV} = 240\angle 0^{\circ} + 12.5\angle 0^{\circ} \times 5.89\angle 89.53^{\circ} = 240.6 + j73.62 = 251.61\angle 17.01^{\circ}$$

Therefore, the magnitude and phase of the inverter voltage is 251.61 and 17.01°.

1.3 Verification of the above designs

To verify this design, the simulation model is built as shown in Figure 1.3. Figures 1.4,1.5,1.6 show results of the AC volatge, AC current and power injected into the AC grid respectively.

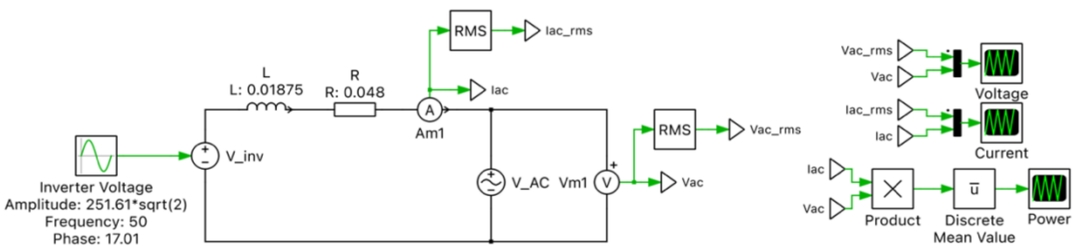

Figure 1.3: Simulation model based on the design

The results that can be observed from the below figures are that when the simulation reaches a steady state: The peak value of AC voltage is around $\pm$340V which is in line with the expectation of 240 V RMS voltage. The AC current waveform is in phase with the voltage waveform which indicates that the inverter outputs pure active power which is in line with the design requirement of reactive power of 0. The RMS value is 12.5 A matching the design specification. The power injected into the grid quickly reaches a steady state with a power of 3 kW, consistent with the specification. The stability of the power waveform indicates that the inverter can deliver power to the grid efficiently with no significant power fluctuations or interruptions.

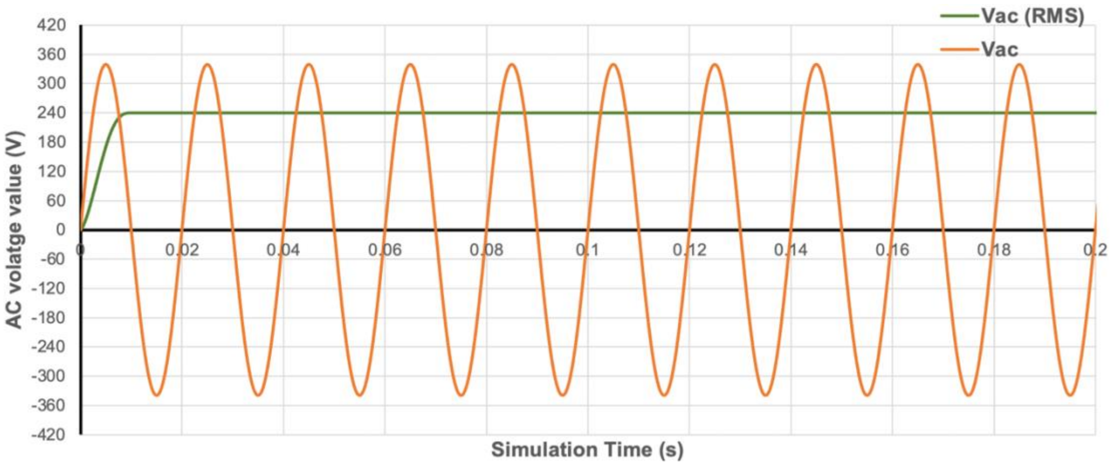

Figure 1.4: Simulation result for AC voltage

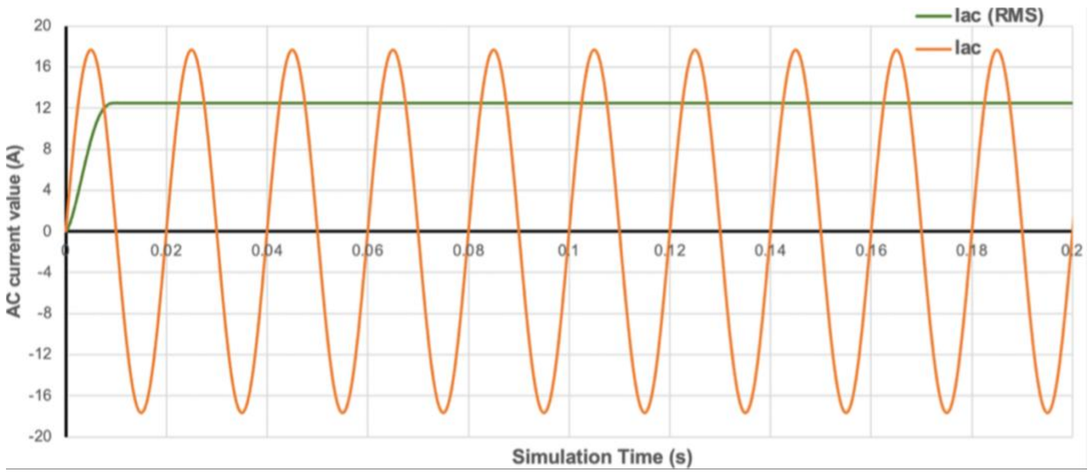

Figure 1.5: Simulation result for AC current

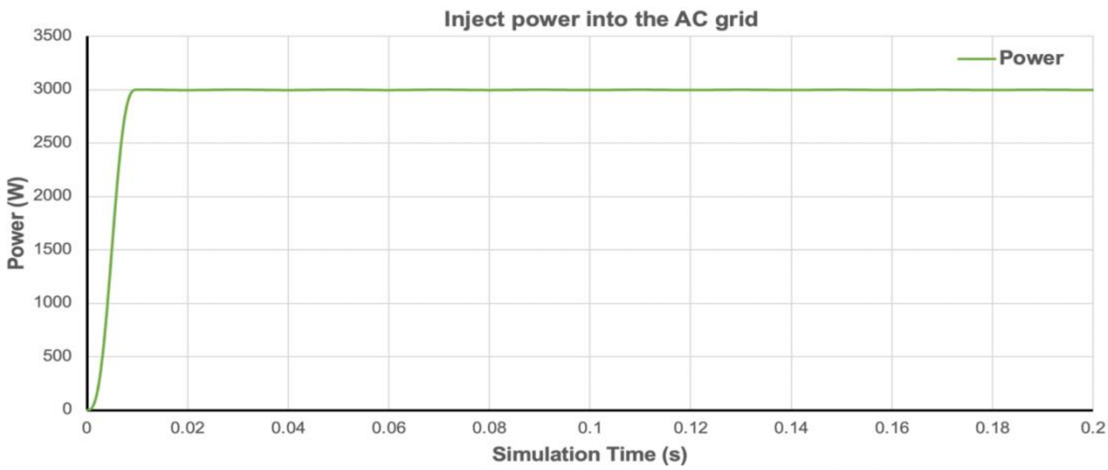

Figure 1.6: Simulation result for power injected into the AC grid

However, the design of the inductor in the filter at this stage is only a preliminary estimate, which means that it may not be completely accurate, but it is sufficient as a starting point for the design.

2. Current Controller Design

The main objective of this section is to design and validate the transfer function of the current controller, which is an important component of a power electronic system used to ensure that the output current of the inverter meets specific performance requirements. There are two subsections, firstly deriving the transfer function of the current loop controller and designing a Proportional Integral (PI) controller. Then, different tools are used to verify transfer functions.

2.1 Find the transfer function of the current loop controller

The first step is to find out the transfer function of the plant. In the control system design, the AC current (I_{AC}) output from the inverter needs to be precisely regulated to synchronise with the grid voltage (V_{AC}) while reacting to changes in the inverter voltage (V_{INV}). To achieve this goal, a mathematical model in the frequency domain is established by taking the difference between the inverter voltage and the grid voltage as input and the AC current generated by the inverter as output, which is shown in Eqn 2.1. Substituting Eqn 1.5 and 1.6 allows this equation to be expressed in concrete data. Figure 2.1 shows the block diagram of the plant obtained from the result of equation.

$$G_p(s) = \frac{I_{AC}(s)}{V_{INV}(s)-V_{AC}(s)} = \frac{1}{Z} = \frac{1}{R+sL} = \frac{1}{0.048+0.01875s} \qquad \textbf{Eqn 2.1}$$

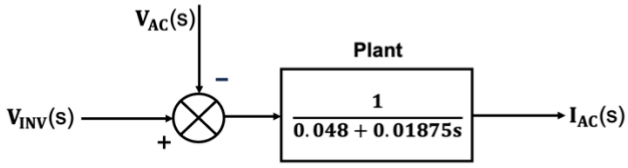

Figure 2.1: The block diagram of the plant

Figure 2.2 shows the overall block diagram for the current controller. The purpose of the controller is to regulate the inverter voltage (V_{INV}) to reduce the error between the reference current (I_{ref}) and the actual current (I_{AC}).

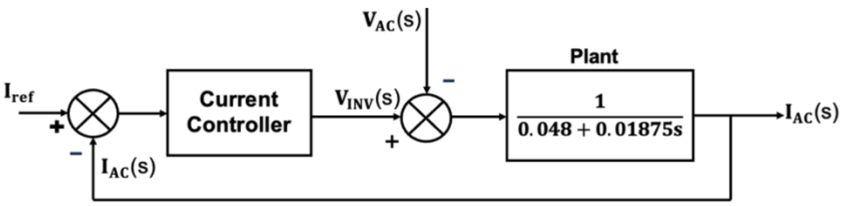

Figure 2.2: The overall block diagram of the current controller

Since plant is a first order response system, it is a good choice to use PI control here, this equation is written in Eqn 2.2. Thus, the open loop equation for this control system can be Eqn 2.3. Since this system has unity gain, the closed loop equation can be written as Eqn 2.4.

$$G_c(s) = K_p + \frac{K_i}{s} \qquad \textbf{Eqn 2.2}$$

$$G_0(s) = G_c(s)G_p(s) = (K_p + \frac{K_i}{s})(\frac{1}{R+sL}) \qquad \textbf{Eqn 2.3}$$

$$G(s) = \frac{G_0(s)}{1+G_0(s)} = \frac{(K_p+\frac{K_i}{s})(\frac{1}{R+sL})}{1+(K_p+\frac{K_i}{s})(\frac{1}{R+sL})} = \frac{\frac{K_p}{L}s+\frac{K_i}{L}}{s^2+\left(\frac{K_p+R}{L}\right)s+\frac{K_i}{L}} \qquad \textbf{Eqn 2.4}$$

Eqn 2.5 is the representation of the denominator in the second order transfer function. Bringing the denominator from Eqn 2.4 into Eqn 2.5 gives the expression for K_p, K_i as shown below. Where ζ is the damping factor which determines the degree of overshoot in the step response, this value is taken as 0.707 here as it allows for a balance between critical damping and under damping, providing a maximally flat system response while maintaining the response speed without excessive oscillations. [2] ω_o is the natural frequency, it can determine the speed of the response. Its value needs to satisfy the Eqn 2.6, where t_s is the settling time and it is also the time to reach 2% reference. According to Eqn 2.6, the value of ω_o can be calculated and thus the values of K_p and K_i can also be obtained. The transfer funtion of the current controller can be represented as Eqn 2.7:

$$s^2 + 2\zeta\omega_o s + \omega_o{}^2 \qquad \textbf{Eqn 2.5}$$

$$\begin{cases} 2\zeta\omega_o = \frac{K_p+R}{L} \\ \omega_o{}^2 = \frac{K_i}{L} \end{cases} \rightarrow \begin{cases} K_p = 2\zeta\omega_o L - R \\ K_i = \omega_o{}^2 L \end{cases}$$

$$t_s = 4T' = \frac{4}{\zeta\omega_o} = 1.5\text{ ms} \qquad \textbf{Eqn 2.6}$$

$$\omega_o = \frac{4}{\zeta t_s} = \frac{4}{0.707\times 1.5\text{ ms}} = 3771.81\text{ rad/s}$$

$$\begin{cases} K_p = 2\times 0.707\times 3771.81\text{ rad/s}\times 18.75\text{ mH} - 0.048\ \Omega = 99.96 \\ K_i = (3771.81\text{ rad/s})^2\times 18.75\text{ mH} = 266747.83 \end{cases}$$

$$G_c(s) = K_p + \frac{K_i}{s} = 99.96 + \frac{266747.83}{s} = \frac{99.96(s+2668.55)}{s} \qquad \textbf{Eqn 2.7}$$

There are several reasons why a PI controller was chosen here [3]:

1) **Elimination of Steady State Errors:** first order systems often have errors at steady state, the integral portion of the PI controller accumulates the error and provides a growing control action until the error is zero, which eliminates the steady state error.
2) **Fast Response:** Proportional control enables the system to respond quickly to deviations and reduces the time it takes to reach a predetermined output.
3) **Improved transition performance:** Integral action reduces oscillations during transitions and speeds the system to a new steady state value. This is an important feature for first order systems that require precise control.
4) **Simplicity and Efficiency:** For first order systems, PI controllers provide a simple and efficient solution. Parameter tuning is relatively simple compared to PID or PD control.

2.2 Verify the transfer function of the current loop controller

To verify this transfer function, "sisotool" of Matlab is used here. "sisotool" allows the user to design various controllers and observe in real time the impact of parameter changes on system performance, thus helping to analyse system stability and determine stability margins.

The steps for verification are as follows: Firstly, "sisotool" is called for the plant function ($G_p(s)$) that needs to be controlled. Second, add integrator and real zero to the Root Locus Editor to satisfy the basic equation for PI control. Third, add the values of settling time (1.5 ms) and damping factor (0.707) to the editor that matches the design specification. Fourth, drag zero to the straight line of settling time and poles to the intersection of the damping factor straight line and the settling time straight line. As shown in Figure 2.3, the black lines are the damping factor and settling time that meet the design requirements, and the zeros and poles have been dragged to their corresponding points.

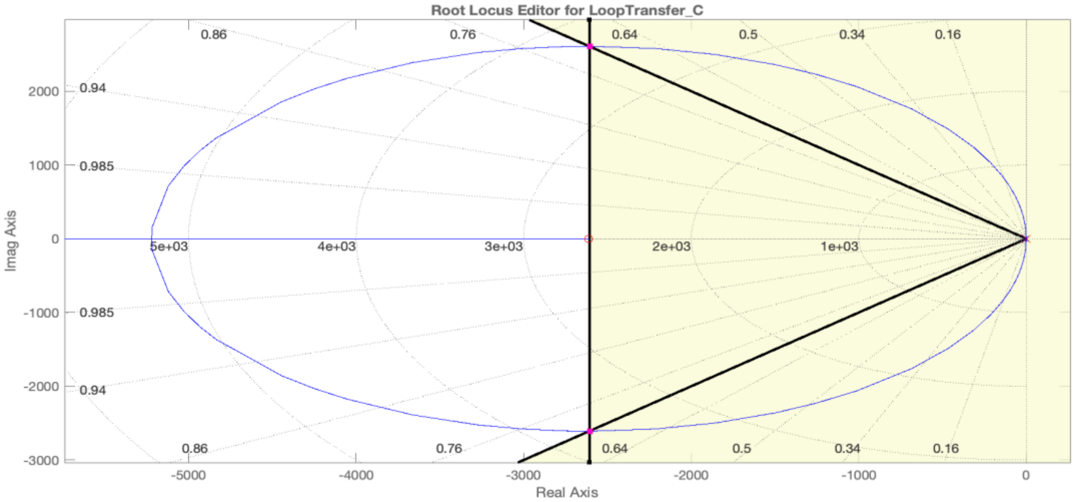

Figure 2.3: The Root Locus Editor for the current controller

The value of G_c read from Matlab is shown below, which is close to the result obtained in the calculation. Since this value is only an approximation obtained by observing the intersection points, it is not accurate and the results from the calculations are used in subsequent simulations.

$$G_c\_Matlab(s) = \frac{97.78(s + 2611)}{s}$$

To better verify that the calculated values satisfy the specification, the designed current controller was simulated on PLECs as shown in Figure 2.4. A signal was input at 0.5 s and the result is shown in Figure 2.5. It can be noticed that the system stabilises within 1.5 ms, which satisfies the previous design (settling time < 1.5 ms).

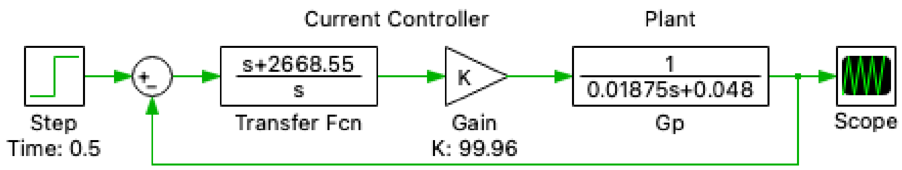

Figure 2.4: The Root Locus Editor for controller

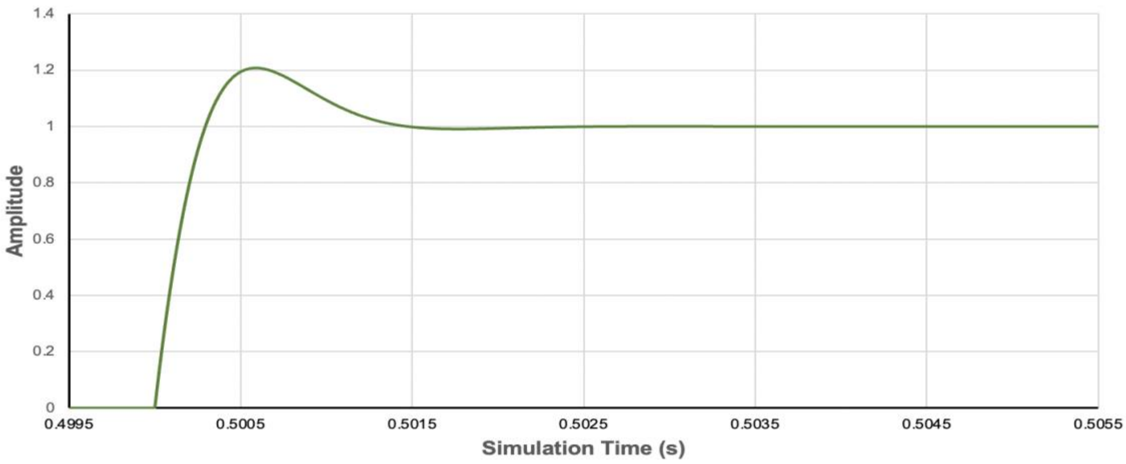

Figure 2.5: The Root Locus Editor for controller

3. Average Model Simulative Verification

There are two subsections in this section, firstly the previously designed current controller is added to the average model, and subsequently the model is subjected to a power step test to determine whether the designed controller performs well.

3.1 Average model of current controller

Figure 3.1 shows the average model with the addition of the current controller, and the roles of the different parts of the model are described below:

1) **AC current reference calculation:** This section calculates the AC current reference (I_{ref}) based on the power to be injected or absorbed. It receives three signals (corresponding to different power levels) and sums them to generate the desired current level. It is multiplied by a sinusoidal waveform to produce the actual reference waveform of the AC current. The amplitude of the sine wave is given by multiplying $\sqrt{2}$ by the RMS value and the frequency is set to 50 Hz, which matches the grid frequency.
2) **Current controller:** It compares the reference current (I_{ref}) with the actual current (I_{ac}) to obtain a current error signal. This error signal is fed into a controller with proportional-integral (PI) action to generate a control signal (V_{inv}). It adjusts the output of the inverter to reduce current errors.
3) **Inverter regulation and feedback loop:** The adjusted inverter output voltage (V_{inv}) affects the current on the load side of the inverter. The actual load current (I_{ac}) is fed back to the controller to form a closed loop control.
4) **Measurements:** To illustrate the subsequent discussion, there are three measurements, power, a comparison of current (I_{ac} and I_{ref}) and a comparison of voltage (V_{inv} and V_{ac}).

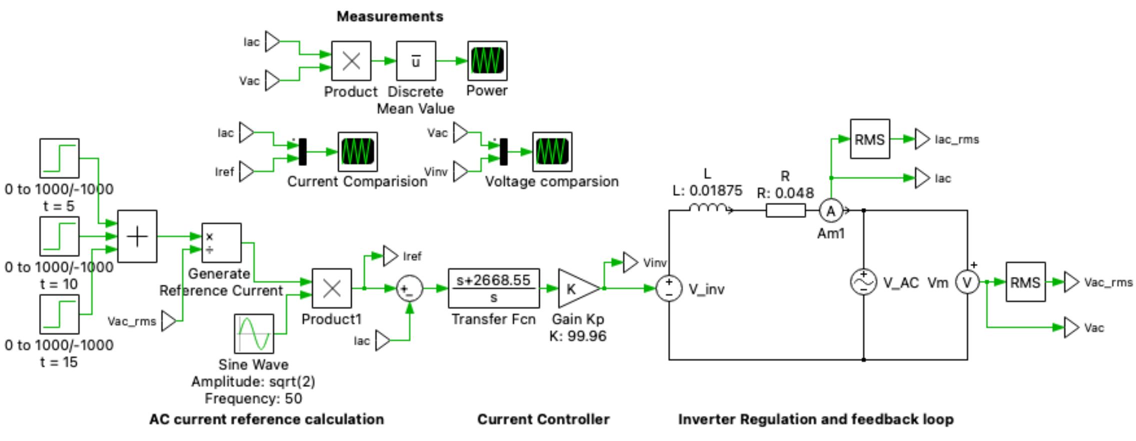

Figure 3.1: Average model of current controller

3.2 Power step testing

Based on the model in Figure 3.1, the result of the model under absorption and transmission of power, and the limitations of the model are discussed below through three aspects:

1) **Power analysis:** Figures 3.2 and 3.3 show the simulation results of injecting/absorbing different power levels into/from the grid, respectively. It can be observed that there are clear jumps in power when the system applies different power levels. These jumps are almost in line with the expected values as shown in Table 1, and the error values are all within 1.5 %. The power reaches the new steady state without excessive oscillation.

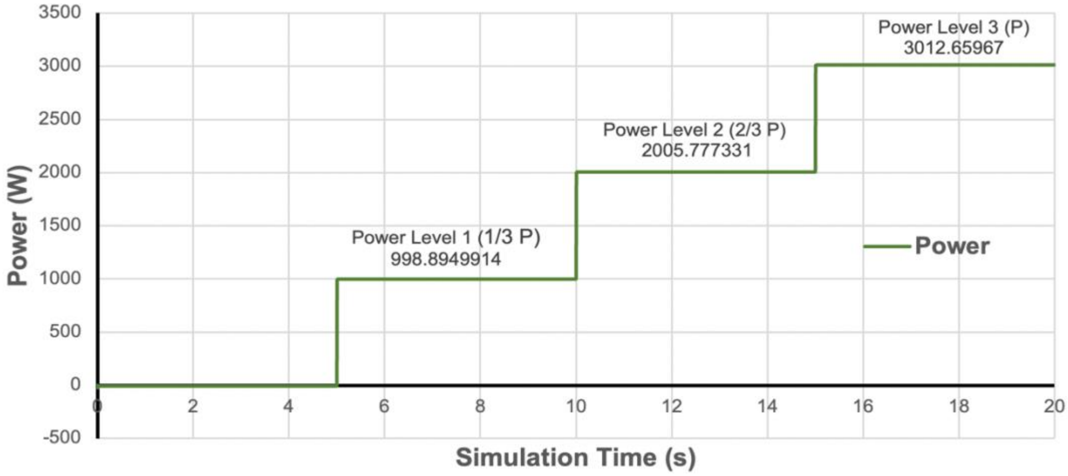

Figure 3.2: Injecting different levels of power into the grid

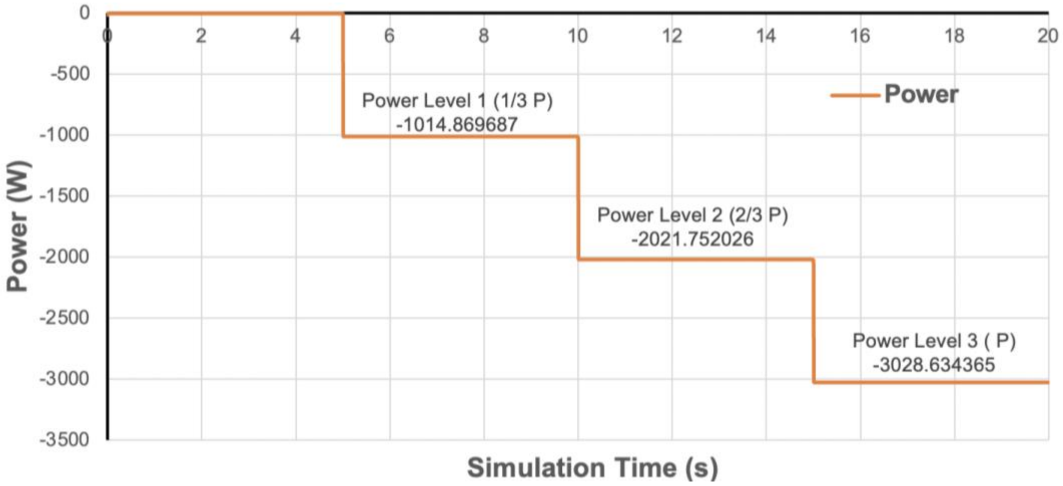

Figure 3.3: Absorbing different levels of power from the grid

Table 1: Comparison of expected and actual power step

	Inject power into the gird			Absorb power from the grid		
	Expect (W)	Actual (W)	Error (%)	Expect (W)	Actual (W)	Error (%)
Power Level 1	1000	998.89	0.11	-1000	-1014.87	1.49
Power Level 2	2000	2005.78	0.29	-2000	-2021.75	1.09
Power Level 3	3000	3012.66	0.42	-3000	-3028.63	0.96

2) **Current tracking performance**: Figures 3.4, 3.5 show the comparison between the reference current (I_{ref}) and the AC grid current (I_{ac}) at different power step articulation points. (Injecting/ Absorbing power) The difference between the two currents represents the error that needs to be adjusted by controller. The goal of an ideal controller is to reduce the steady state error to zero or near zero. From the figures, it can be noticed that the amplitude of the two current waveforms is almost the same and the phases are nearly aligned. When changing to a different power level, I_{ref} can jump to the value corresponding to the new power level, and I_{AC} follows this change quickly and smoothly. This means that the parameters (K_p, K_i) previously chosen for the PI controller are very efficient values, allowing the system to respond precisely to a given command without excessive delays.

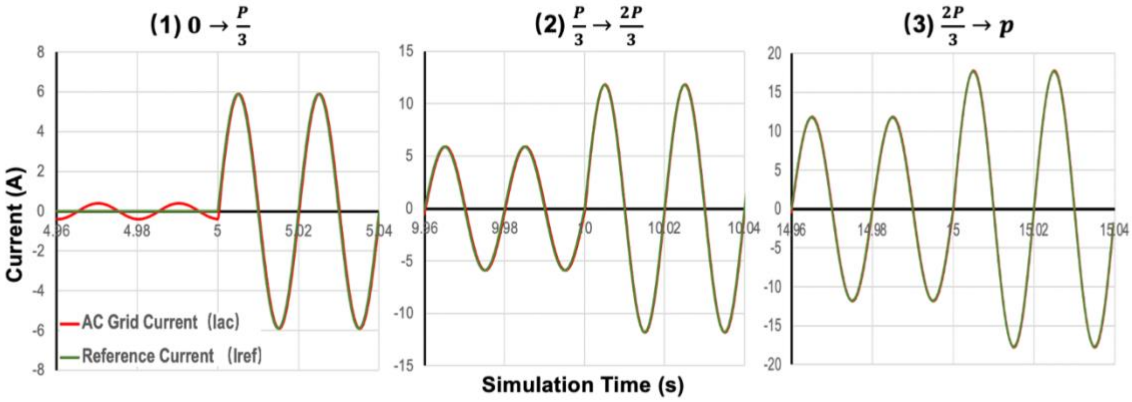

Figure 3.4: Compare I_{ref} and I_{ac} at different power step articulation points (Injecting power)

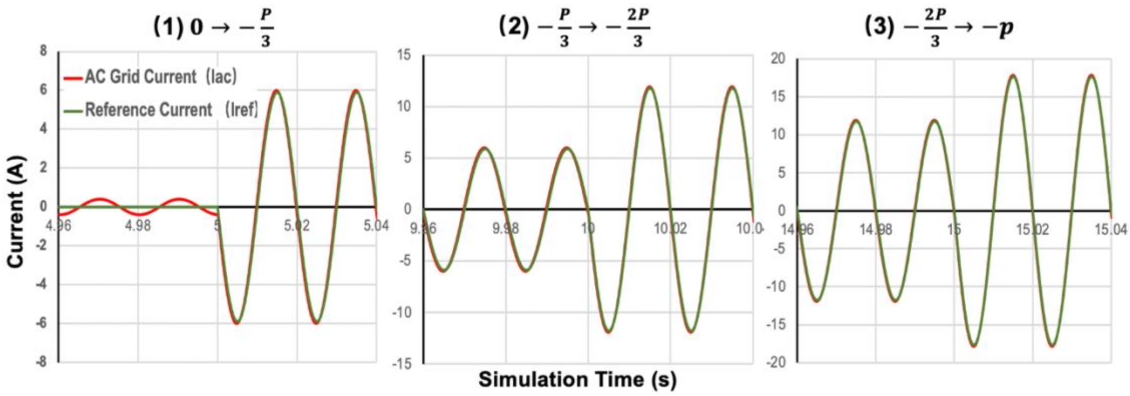

Figure 3.5: Compare I_{ref} and I_{ac} at different power step articulation points (Absorbing power)

To better analyse the performance of the current tracking, Figure 3.6 shows the results using the FFT for the two currents, it can be noticed that the main peaks of the two currents are located at the same frequency (50 Hz) and the peaks at the other frequencies are very low or close to zero, this indicates that the reference current is being tracked accurately and does not show any additional frequency components. However, it can be noticed that the peaks of the two currents are not perfectly aligned and there is a frequency deviation or phase shift. This means that the controller may not have been able to eliminate errors in the current waveform, resulting in the actual current not accurately replicating the reference current.

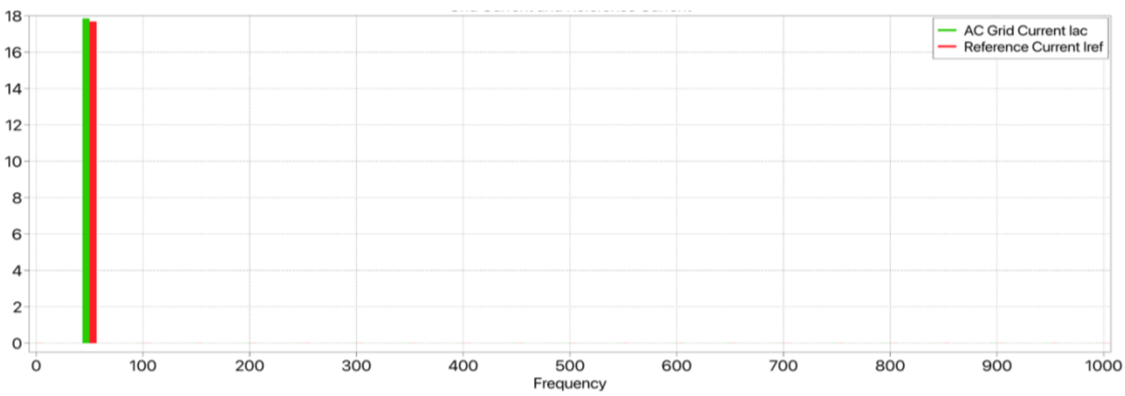

Figure 3.6: FFT analysis for I_{ref} and I_{ac}

3) **Voltage phase and amplitude**: Figure 3.7 and 3.8 shows comparison between the inverter voltage (V_{inv}) and the AC grid voltage (V_{AC}) for the last power step stage (P = 3000 W). Figure 3.7 shows the case of injected power and the labelled peak V_{inv} is approximately

358.24 V and Figure 3.8 shows the case of absorbed power and the labelled peak V_{inv} is approximately 356.51V. From the design of the first part, the expected value of V_{inv} should be at 355.83 V ($252.61 \times \sqrt{2}$). Figures 3.7 and 3.8 show a larger result, which indicates that the output of the controller is slightly inaccurate and does not achieve precise control. In addition, the final output power is larger than expected, the reason for this may be that the phase difference between V_{inv} and V_{ac} is different from what was envisaged in the first part (17.01°). A small phase difference can have a noticeable effect on power.

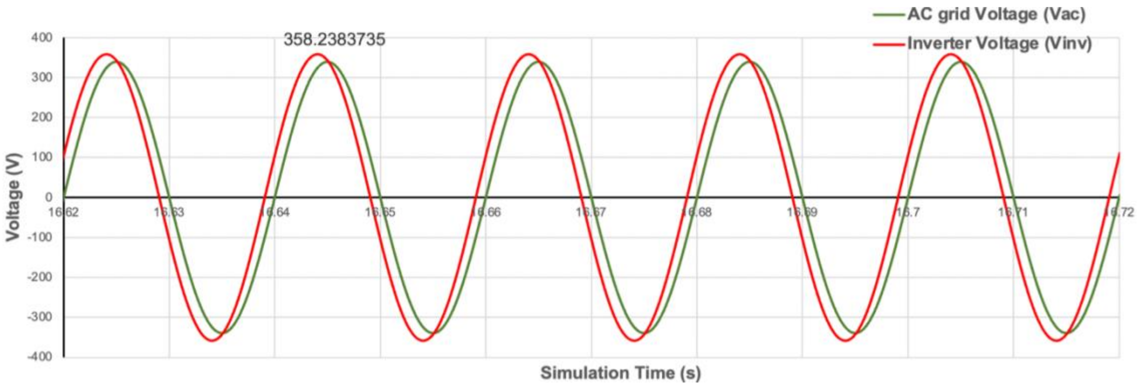

Figure 3.7: Comparison between V_{inv} and V_{AC} (Injecting power)

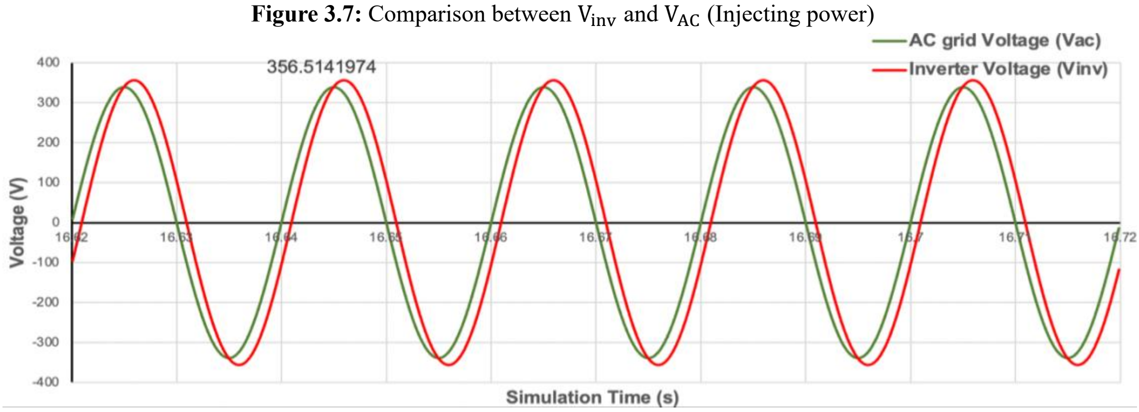

Figure 3.8: Comparison between V_{inv} and V_{AC} (Absorbing power)

Based on the results discussed above, it can be found that the designed PI controller still has some limitations and defects:

1) **Inadequate Parameter Adjustment:** K_p, K_i may not be properly adjusted, resulting in inaccurate controller response. The controller may have over-amplified the error, causing the inverter output voltage to be too high, which in turn increases the output power. Also, defective parameters can prevent the PI controller from providing a fast enough response to ensure synchronisation under changing load or reference conditions.
2) **Integral Windup** [4]**:** when the integral term (K_i) accumulates too much error, especially in the presence of large setpoint variations or persistent errors, this may cause the controller output to saturate, resulting in high V_{inv} and I_{ac}.
3) **Non-linearities not considered:** PI controller usually assumes that the system is linear [5], and if the system exhibits significant non-linear characteristics (when non-linear components are subsequently added), the effectiveness of the PI controller can be reduced.
4) **No differential control:** PI controller lacks a differential term, which means that it cannot predict future trends in system error and adjust in advance. PID controller, through its differential term, can improve the response speed of the system and reduce phase delays. [5]

4. Capacitor Design and Voltage Controller Designing

Voltage controllers are designed to ensure that the DC side voltage of a PV system is maintained at a stable reference value. This is essential to ensure that the inverter can efficiently convert DC power into stable AC power to meet the requirements of the grid. Here are three subsections for designing the capacitor, voltage controller and verifying the controller.

4.1 Design capacitor based on the specification

There is a DC-link capacitor between the DC power supply and the inverter. It is mainly used to store energy and smooth out DC voltage ripple. It allows AC current to flow and blocks DC current. It stabilises the power supply, optimises the performance of the inverter and improves the response of the system to changes in load. Eqn 4.1 is used to calculate it that can be achieved the desired voltage ripple. The ripple here is the half of the DC voltage ripple (peak-peak), which is 0.25 V.

$$C = \frac{\hat{V}_{AC}\hat{I}_{AC}}{4\omega V_{DC}\hat{V}_{DC}^{ripple}} = \frac{\sqrt{2}\times 240\ \mathrm{V}\times\sqrt{2}\times 12.5\ \mathrm{A}}{4\times 2\pi\times 50\ \mathrm{Hz}\times 600\ \mathrm{V}\times 0.25\ \mathrm{V}} = 31.83\ \mathrm{mF} \qquad \textbf{Eqn 4.1}$$

4.2 Find the transfer function of the voltage controller

The first step is to derive the plant transfer function of the voltage controller. Eqn 4.2 shows the relationship between the energy stored in the capacitor and the voltage. To facilitate the analysis of the control system, the energy relationship is applied the Laplace transform and the process is shown below. P_c is the difference between the PV power (P_{PV}) and the AC load power (P_{AC}) and the equation can be written as Eqn 4.3. By rearranging the equation, the transfer function of the plant can be obtained as Eqn 4.4. Figure 4.1 illustrates the block diagram of the plant.

$$E_c(t) = \frac{1}{2}CV_{DC}(t)^2 \qquad \textbf{Eqn 4.2}$$

$$V_{DC}(t)^2 = \frac{2}{C}E_c(t) \rightarrow V_{DC}(s)^2 = \frac{2}{C}E_c(s) \rightarrow V_{DC}(s)^2 = \frac{2}{C}\frac{1}{s}P_c(s) = \frac{2}{sC}P_c(s)$$

$$V_{DC}(s)^2 = \frac{2}{sC}(P_{PV}(s) - P_{AC}(s)) \qquad \textbf{Eqn 4.3}$$

$$G_P(s) = \frac{V_{DC}(s)^2}{(P_{PV}(s) - P_{AC}(s))} = \frac{2}{sC} = \frac{2}{s\times 31.83\ \mathrm{mF}} = \frac{62.83}{s} \qquad \textbf{Eqn 4.4}$$

Figure 4.1: The block diagram of the plant for the voltage controller

Figure 4.2 shows the overall block diagram for the voltage controller. The input signal is the square of the reference DC voltage ($(V_{DC}ref)^2$) and the square of the actual DC voltage ($(V_{DC})^2$), and the error signal of the controller is the subtraction of these two signals.

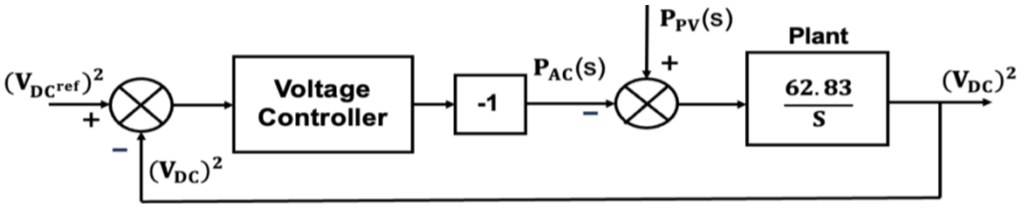

Figure 4.2: The overall block diagram of the voltage controller

Since the plant here is also a first order response system, PI control is also used like current controller. Hence the open loop equation for this control system is Eqn 4.5. since this system has single gain, the closed loop equation can be written as Eqn 4.6. The expressions for K_p, K_i were also solved using Eqn 2.5.

$$G_0(s) = G_c(s)G_p(s) = (K_p + \frac{K_i}{s})(\frac{2}{sC}) \qquad \textbf{Eqn 4.5}$$

$$G(s) = \frac{G_0(s)}{1+G_0(s)} = \frac{(K_p+\frac{K_i}{s})(\frac{2}{sC})}{1+(K_p+\frac{K_i}{s})(\frac{2}{sC})} = \frac{\frac{2K_p}{C}s+\frac{2K_i}{C}}{s^2+\frac{2K_p}{C}s+\frac{2K_i}{C}} \qquad \textbf{Eqn 4.6}$$

$$\begin{cases} 2\zeta\omega_o = \frac{2K_p}{C} \\ {\omega_o}^2 = \frac{2K_i}{C} \end{cases} \rightarrow \begin{cases} K_p = \zeta\omega_o C \\ K_i = \frac{{\omega_o}^2 C}{2} \end{cases}$$

In this system, the current controller is described as the "inner loop" and the voltage controller as the "outer loop", usually the inner loop has a shorter response time than the outer loop because the inner loop needs to react quickly to any disturbances and maintain stability. Therefore, the voltage controller setting time should be slower than the current controller, which is set to 10 ms. Therefore, the natural frequency required here is also different, and the damping factor is also 0.707. Based on Eqn 2.6, the calculation of the natural frequency is as follows. Thus, the value of K_p and K_i can also be obtained. The transfer funtion of the current controller can be represented as Eqn 4.7:

$$\omega_o = \frac{4}{\zeta t_s} = \frac{4}{0.707\times 10\ \text{ms}} = 565.77\ \text{rad/s}$$

$$\begin{cases} K_p = 0.707\times 565.77\ \text{rad/s}\times 31.83\ \text{mF} = 12.73 \\ K_i = \frac{(565.77\ \text{rad/s})^2\times 31.83\ \text{mF}}{2} = 5094.32 \end{cases}$$

$$G_c(s) = K_p + \frac{K_i}{s} = 12.73 + \frac{5094.32}{s} = \frac{12.43(s+400.1)}{s} \qquad \textbf{Eqn 4.7}$$

4.3 Verify the transfer function of the voltage controller

Here the transfer function is still verified by sisotool, the method is the same as the current controller, except that the settling time is set to 10 ms. The result is shown in Figure 4.3. The transfer function that can be read from this figure is shown below, which is close to the calculated result. Subsequent simulations continue to use calculated values due to possible.

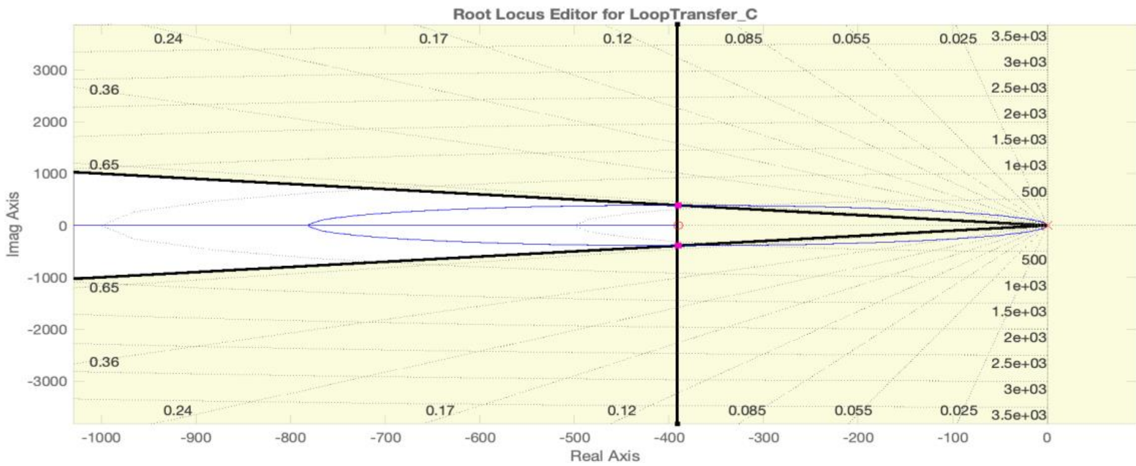

Figure 4.3: The Root Locus Editor for the volage controller

$$G_c\_Matlab(s) = \frac{12.43(s+390.5)}{s}$$

Figure 4.4 shows the voltage controller designed based on the data calculated above, since there is no actual inverter in this circuit, the transfer function of the capacitor is used to replace the role of the capacitor in the circuit. Figure 4.5 shows a comparison between its output DC voltage (V_{dc}) and the reference DC voltage ($V_{dc}{}^{ref}$) for evaluating the performance of this controller. V_{dc} rises rapidly at the start of the simulation, with overshoot, and does not fully reach a stable 600 V within 10 ms. The reason for this may be related to the limitations of the controller used in this stage: The choice of controller parameters was based on simplified models or empirical formulae for adjustment without adequate dynamic testing, resulting in poor performance. In addition, simple PI control may not be suitable for this system, and it may be necessary to introduce differential control (PID controller) or use more advanced control strategies to meet the performance requirements. [5]

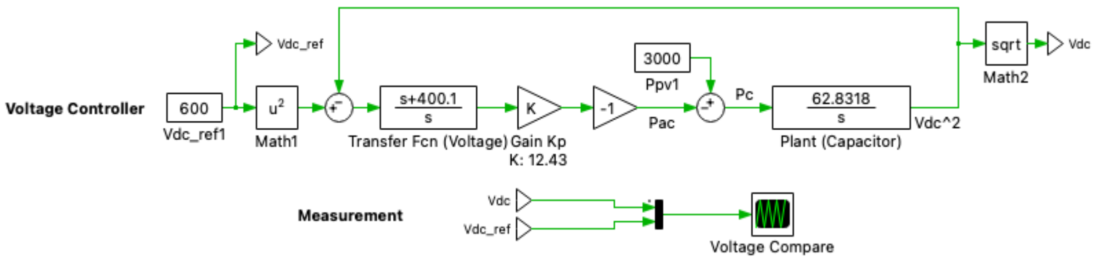

Figure 4.4: Average model of voltage controller

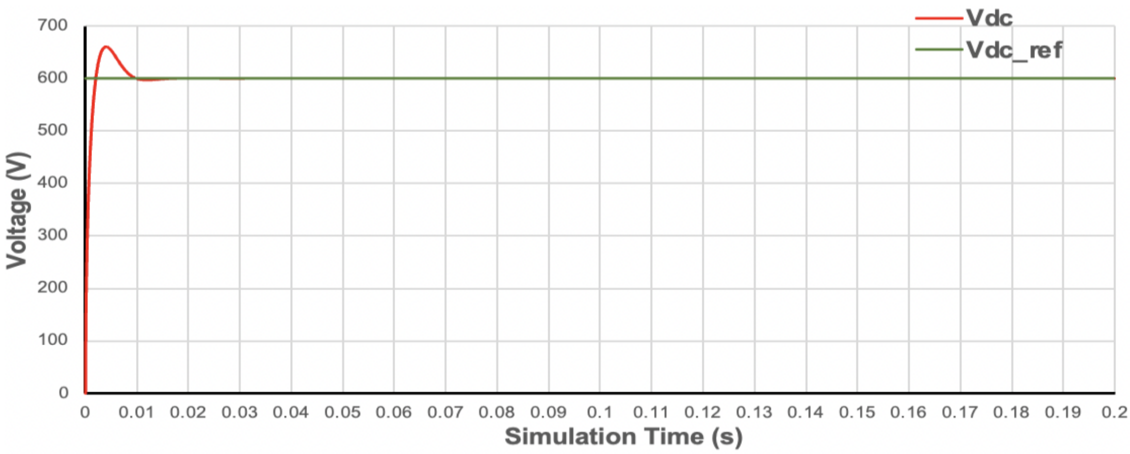

Figure 4.5: The DC Voltage transient states

5. Full Average Model Analysis

This section includes combining all the previous designs, the first subsection is the description of the model, and the second subsection is the analysis of its results.

5.1 Full Average model

Figure 5.1 shows that in combination with the previously designed full average model, the voltage controller outputs a control signal which is based on the DC voltage reference and the voltage feedback from the system. This control signal is used as a reference current (I_{ref}) for the current controller, which in turn adjusts the output of the inverter to maintain this reference current. The output of the current controller in turn affects the switching state of the inverter, thus indirectly controlling the AC voltage and current.

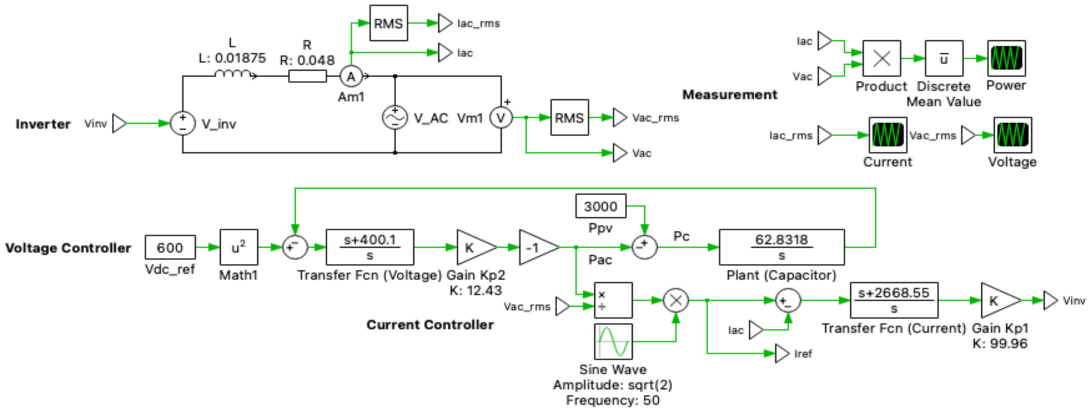

Figure 5.1: Full average model

5.2 Results of full average model

Figures 5.2, 5.3 and 5.4 show the full average model output, power, I_{ac} and V_{ac} respectively. (For power and current, the original simulation is shown on the left, and a zoomed-in view of the steady-state simulation results is shown on the right.) It can be found that the power first drops to a negative value and then increases to about 2×10^5 W, finally stabilised at 3012 W. The reason why this value is higher than 3000 W was also analysed in part 2 (Current controller Design). AC current curve first increases to 2×10^5 A and then stabilizes at about 12.5 A, which is as expected. AC voltage stabilizes at 240 V after some time, which is also as expected.

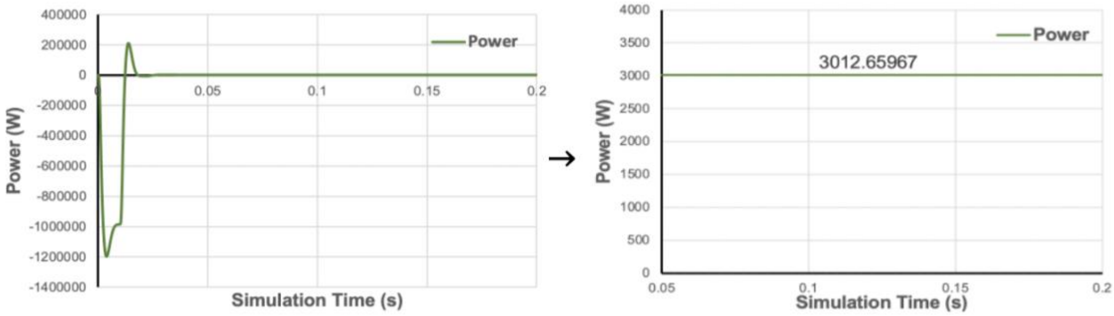

Figure 5.2: Simulation result for power injected into the AC grid

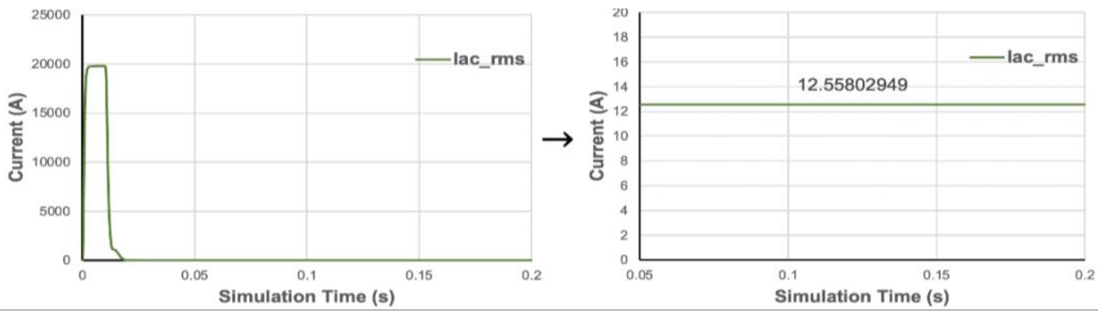

Figure 5.3: Simulation result for AC current

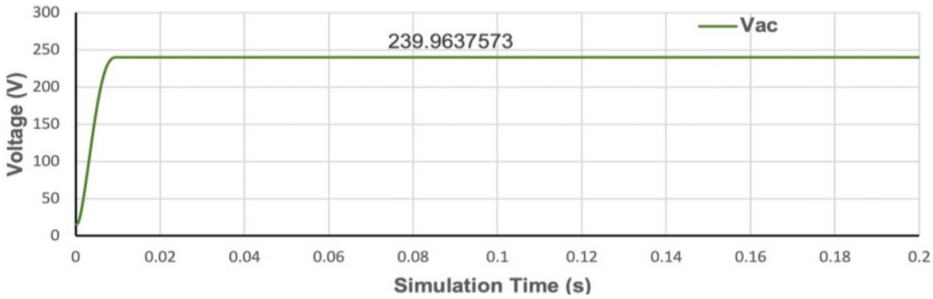

Figure 5.4: Simulation result for AC voltage

Possible reasons for the negative and overshoot curve are:

1) **Settling time of the voltage controller:** The settling time of the voltage controller may not be set properly. As mentioned in the fourth part of the design, if the settling time of the voltage controller is smaller than that of the current controller, the voltage controller may over-regulate based on an inaccurate current setpoint, resulting in an unstable system. However, if the settling time is too large it can also lead to a larger overshoot in the final output [6], so how to weigh the value of settling time has also become a difficult point.
2) **Control system dynamics:** The control system may take some time to "learn" how to handle load changes, especially when the system is first started up. [7] If the parameters of the PI controller are not properly adjusted, the system may not be able to properly adjust to the setpoint. This may result in overshoot and undershoot before the system reaches steady state.

6. Conclusion

In conclusion, this report effectively demonstrates a thorough approach to designing an inverter system. It encompasses detailed methodologies for the design and verification of LR filter, current and voltage controllers, and the integration of these into a full average model. There are some small errors in the output, but the results are basically as expected. For current controller, there is a need to improve its PI design. It faces challenges in parameter tuning and is prone to problems such as integral rise, which suggests the need for more advanced adaptive control strategies for more accurate current regulation. Similarly, the voltage controller, which is critical for maintaining a stable DC-side voltage, can be improved by modifying its settling time to prevent excessive output overshoot. This may involve integrating more sophisticated control methods such as PID control or advanced algorithms that consider system nonlinearities.

7. Reference

[1] Y. Tang, S. Xie, and J. Ding, "Pulsewidth modulation of Z-source inverters with minimum inductor current ripple," IEEE Transactions on Industrial Electronics, vol. 61, no. 1, pp. 98-106, 2013.

[2] A. M. Diab et al., "Fast and simple tuning rules of synchronous reference frame proportional-integral current controller," IEEE Access, vol. 9, pp. 22156-22170, 2021.

[3] M. Roslan, A. Q. Al-Shetwi, M. Hannan, P. Ker, and A. Zuhdi, "Particle swarm optimization algorithm-based PI inverter controller for a grid-connected PV system," PloS one, vol. 15, no. 12, p. e0243581, 2020.

[4] X.-l. Li, J.-G. Park, and H.-B. Shin, "Comparison and evaluation of anti-windup PI controllers," Journal of Power Electronics, vol. 11, no. 1, pp. 45-50, 2011

[5] S. Alqahtani, S. Ganesan, and M. A. Zohdy, "The Comparison between PI and PID Controllers in Engine Speed Control Model," in 2020 IEEE International Conference on Electro Information Technology (EIT), 2020: IEEE, pp. 629-634.

[6] A. G. Yepes, A. Vidal, J. Malvar, O. López, and J. Doval-Gandoy, "Tuning method aimed at optimized settling time and overshoot for synchronous proportional-integral current control in electric machines," IEEE Transactions on Power Electronics, vol. 29, no. 6, pp. 3041-3054, 2013.

[7] T. Yang, L. Zhao, W. Li, and A. Y. Zomaya, "Reinforcement learning in sustainable energy and electric systems: A survey," Annual Reviews in Control, vol. 49, pp. 145-163, 2020.